

discoveries appear to be the first example of refuge facilitation in primary succession after a major natural disturbance. This process may commonly contribute to regrowth of kelp (21).

LARRY G. HARRIS

Department of Zoology, University of
New Hampshire, Durham 03824

ALFRED W. EBELING

DAVID R. LAUR

ROBERT J. ROWLEY

Department of Biological Sciences and
Marine Science Institute, University
of California, Santa Barbara 93106

References and Notes

1. F. E. Clements, *Carnegie Inst. Washington Publ.* **242**, 1 (1916); F. L. Golley, *Ecological Succession* (Dowden, Hutchinson, and Ross, Stroudsburg, Pa., 1977); H. S. Horn, in *Theoretical Ecology*, R. M. May, Ed. (Sinauer, Sunderland, Mass., ed. 2, 1981), p. 253; E. P. Odum, *Science* **164**, 262 (1969).
2. J. H. Connell and R. O. Slatyer, *Am. Nat.* **111**, 1119 (1977).
3. C. A. Simenstad, J. A. Estes, K. W. Kenyon, *Science* **200**, 403 (1978).
4. T. F. Goreau, *Ecology* **40**, 67 (1959); J. D. Woodley et al., *Science* **214**, 749 (1981); R. K. Cowen, C. R. Agegian, M. S. Foster, *J. Exp. Mar. Biol. Ecol.* **64**, 189 (1982).
5. A. W. Ebeling, D. R. Laur, R. J. Rowley, in preparation.
6. P. K. Dayton and M. J. Tegner [*Science* **224**, 283 (1984)] give a general summary of this storm and other effects of the recent strong El Niño climatic anomaly on the Southern California kelp community.
7. New surfaces are surfaces of virgin rock exposed for the first time during the storm; old surfaces are those containing coralline algal crusts, indicating that they had been in place for some period before the storm.
8. W. J. North, *Nova Hedwigia* (Suppl.) **42**, (1971); M. S. Foster, *Mar. Biol.* **32**, 313 (1975); M. Neushul, M. S. Foster, D. A. Coon, J. W. Woessner, B. W. W. Harger, *J. Phycol.* **12**, 397 (1976); B. W. W. Harger, thesis, University of California, Santa Barbara (1979); P. K. Dayton et al., *Ecol. Monogr.*, in press.
9. J. C. Quast [Calif. Dep. Fish Game Fish Bull. **139**, 109 (1968)] found kelp in guts of these fishes.
10. The exceptional treatment was on a surge, exposed slope, which may have discouraged fish grazing.
11. The zone of meristomatic growth is at the junction of sporophyte blade and stipe. Since blades can regenerate from stipes, bladeless stipes may survive.
12. R. R. Sokal and F. J. Rohlf, *Biometry* (Freeman, San Francisco, ed. 2, 1981), p. 737.
13. A sea star (*Patiria miniata*) was found feeding on a patch of new surface and had cleared a swath through the dense stand of filamentous algae, leaving only the kelp sporophytes. All sporophytes in the swath had been cropped down to 4 cm, while the filamentous algae and sporophytes were about 12 cm in height on both sides of the swath.
14. Alternatively, fish may have been attracted by the disturbance of plot manipulation. However, the same grazing differential was observed on the unmanipulated surfaces in quadrat samples.
15. W. L. Montgomery, T. Gerrodette, L. D. Marshall, *Bull. Mar. Sci.* **30**, 901 (1980).
16. Similar differences in sporophyte densities were found between old and new surfaces in permanent quadrats established by D. Laur several years before the storm.
17. W. P. Sousa, *Ecol. Monogr.* **49**, 227 (1979); W. P. Sousa, S. C. Schroeter, S. D. Gaines, *Oecologia* (Berlin) **48**, 279 (1981); D. Breitburg, *Ecology*, in press.
18. T. Turner, *Am. Nat.*, **121**, 729 (1983).
19. B. A. Menge, *Oecologia* (Berlin) **34**, 17 (1978).
20. G. Russ, *J. Exp. Mar. Biol. Ecol.* **42**, 55 (1980); P. S. Petraitis, *Ecology* **64**, 522 (1983).
21. J. S. Stephens, Jr., observed widespread kelp recruitment and survival in dense vegetation on new rock surfaces created off Los Angeles by the 1983 storm, and W. J. North noted that outplanting young kelp among such vegetation may alleviate damage from fish grazing (personal communications).
22. We thank R. Bray, J. C. Connell, M. Hixon, S. Holbrook, R. Larson, R. Schmitt, and J. S. Stephens, Jr. for reviewing the manuscript. Supported by a University of New Hampshire—University of Maine National Oceanic and Atmospheric Administration Sea Grant (L.G.H.) and NSF grant OCE82-08183 (A.W.E. and D.R.L.).

30 January 1984; accepted 24 April 1984

Bishop Tuff Revisited: New Rare Earth Element Data Consistent with Crystal Fractionation

Abstract. *The Bishop Tuff of eastern California is the type example of a high-silica rhyolite that, according to Hildreth, supposedly evolved by liquid-state differentiation. New analyses establish that the Bishop Tuff "early/late" rare earth element trend reported by Hildreth mimics the relations between groundmass glasses and whole rocks for allanite-bearing pumice. Differences in elemental concentrations between whole rock and groundmass are the result of phenocryst precipitation; thus the data of Hildreth are precisely those expected to result from crystal fractionation.*

Considerable interest has been focused recently on the Bishop Tuff because it is the type example of a major high-silica rhyolitic magma that supposedly evolved by liquid-state diffusion. The tuff was the subject of an exhaustive petrologic study by Hildreth (1, 2), who concluded that crystal fractionation played no important role in establishing preeruptive chemical gradients in the Bishop Tuff magma chamber. Hildreth proposed that the magma differentiated in the liquid state, and he coined the term "thermogravitational diffusion" to encompass liquid-state fractionation pro-

cesses such as Soret separation and diffusion of cations complexed with volatile components. Hildreth (3) and Mahood and Hildreth (4) have treated high-silica rhyolites as a class distinct from less silicic rocks because they believe that liquid-state mechanisms played a leading role in the evolution of high-silica rhyolites.

The thermogravitational mechanism is admittedly poorly understood (1-4), and the model is not even qualitatively testable. Rhyolites and granites that supposedly have evolved by liquid-state diffusion are usually identified on the basis of

a comparison of their geochemical enrichment patterns to that of the Bishop Tuff (5). The rare earth element (REE) trends are thought to be especially important in the recognition of rock suites affected by thermogravitational diffusion; in the Bishop Tuff the light REE decrease and the heavy REE increase with diminishing temperature, increasing inferred stratigraphic height, and increasing rock SiO₂ content (1). The material that erupted early is more differentiated than that erupted later, and this is interpreted to represent the inverse stratigraphy of the magma chamber. Criticisms of the liquid state-differentiation model have been based on reinterpretations of Hildreth's data (6) or on studies of granitoids (7). Important experimental studies of Soret diffusion in melts of Bishop Tuff compositions are now in progress but have not yet been published (8).

The data reported here are, to my knowledge, the first new geochemical analyses of the Bishop Tuff to be published since Hildreth's study, and these data are significantly more precise than his. In this study the differentiation of the Bishop Tuff is examined on the least equivocal scale, that of individual hand specimen-sized samples (about 1 kg). For such small-scale samples the differences in REE concentrations between porphyritic whole-rock specimens and their groundmass glasses must reflect crystal-melt processes such as crystal precipitation or accumulation, provided that the effects of alteration are minimal. These concentration differences cannot be the result of thermogravitational diffusion because no significant thermal or gravitational gradient existed on the scale of a hand specimen. Hildreth has detailed (1) several mineralogical arguments that establish that there was no significant crystal settling or accumulation in the Bishop Tuff magma chamber. These groundmass/whole-rock relations, therefore, clearly document the effects of crystal precipitation.

I discuss the samples in the context of Hildreth's (1) temperature stratigraphy. He found that the temperatures of the iron-titanium oxides ranged from 720°C in the early erupted air fall to 790°C in rocks that erupted late. Quartz, sanidine, oligoclase, biotite, ilmenite, titanomagnetite, zircon, and apatite are ubiquitous phenocrysts. Allanite, a light REE-rich mineral of the epidote family, appears at 763°C and is present in all samples of lower temperature.

For this study pumice blocks were collected from three of Hildreth's (2) sample localities that represent nearly

the entire temperature range of the tuff. Temperatures and mineral assemblages referred to here are based on Hildreth's descriptions of the localities (9). The high-temperature sample is allanite-free, whereas the two samples of lower temperature contain allanite. The chemical separations and mass spectroscopy of the REE were done in G. N. Hanson's laboratory at the State University of New York, Stony Brook. Replicate dissolutions and analyses of Bishop Tuff glass (Table 1) and other homogeneous samples indicate a precision of about 1 percent. The precision is not as good (about 5 percent) for europium in sample HB52 because of its very low concentration in this particular sample and an unfavorable spike/sample ratio.

The pumice whole-rock REE trends (Fig. 1A) agree with those reported by Hildreth (1). The heavy REE increase with decreasing temperature. The high- and medium-temperature samples have similar concentrations of light REE, but the low-temperature sample is relatively depleted in the light REE. The low-temperature REE pattern crosses the two higher temperature patterns between neodymium and samarium (Fig. 1A). In the high-temperature sample, the groundmass glass is enriched in all REE except europium with respect to the whole rock (Fig. 1D, Table 1). The heavy REE are, however, enriched far more (about 20 percent) than the light REE [neodymium (about 5 percent) and cerium (about 2½ percent)]. The groundmass glass in the medium- and low-temperature samples, both of which contain allanite, is also enriched (about 20 percent) in the heavy REE with respect to the whole rocks (Fig. 1, B and C; Table 1). These groundmasses, however, are depleted in cerium by 7 to 13 percent with respect to the whole rocks, and the groundmass/whole-rock patterns cross between neodymium and samarium.

The striking feature of the REE patterns in Fig. 1 is that the groundmass/whole-rock relations for the allanite-bearing samples are identical to the Bishop Tuff early/late trend reported by Hildreth (1). Although only three samples were analyzed in this study, they cover the complete range in REE compositions found by Hildreth. Results for the high-temperature sample (Fig. 1D) demonstrate that, even in the absence of allanite, crystal fractionation suppresses enrichment of the light REE. This suppression is the result of the light REE-enriched partition coefficient patterns of the ferromagnesian phenocrysts. Mahood and Hildreth (4) reported that the major ferromagnesian phases in the

Table 1. Rare earth element analysis of Bishop Tuff pumice samples. Results of analyses of separate dissolutions of glass from sample HB52 are shown.

Sample	Concentration (ppm)							
	Ce- rium	Neo- dymium	Samar- ium	Euro- pium	Gado- linium	Dyspro- sium	Er- bium	Ytter- bium
HB77 (790°C)								
Rock	91.6	24.9	2.99	0.336	1.78	1.51	0.912	0.987
Glass	93.9	26.1	3.22	0.235	2.08	1.86	1.10	1.21
HB133 (762°C)								
Rock	89.5	25.3	3.23	0.296	2.12	1.92	1.19	1.24
Glass	83.0	24.5	3.45	0.188	2.34	2.23	1.41	1.45
HB52 (733°C)								
Rock	54.2	19.5	3.70	0.0658	3.00	3.15	1.92	2.04
Glass 1	47.1	18.3	3.90	0.0480	3.39	3.71	2.29	2.42
Glass 2	47.5	18.4	3.89	0.0458	3.40	3.71	2.27	2.39

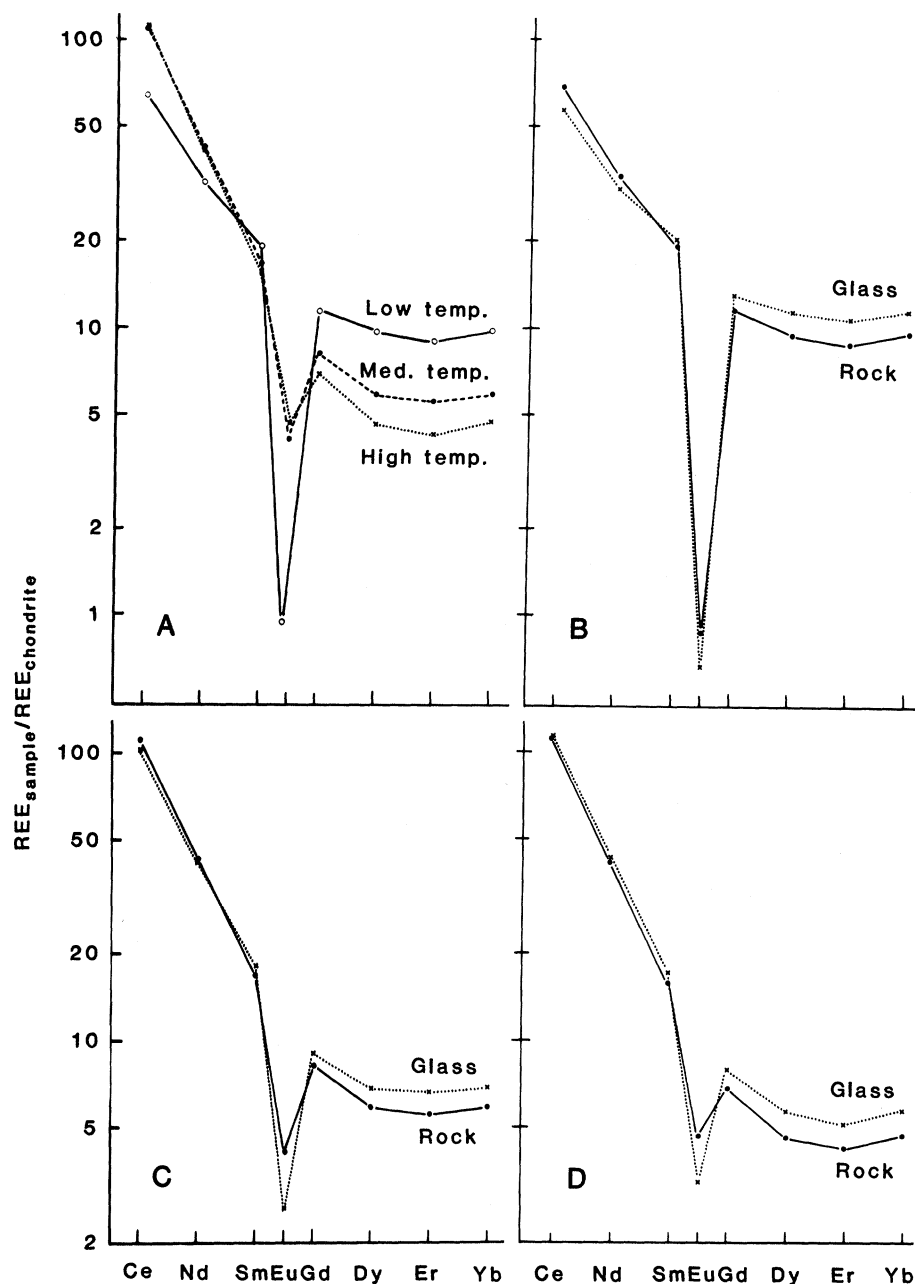


Fig. 1. Chondrite-normalized rare earth element patterns of pumice whole rocks and pumice groundmass glasses from the Bishop Tuff: (A) pumice (rocks); (B) low-temperature, allanite-bearing sample (HB52); (C) medium-temperature, allanite-bearing sample (HB133); and (D) high-temperature, allanite-free sample (HB77). See Table 1 for sample analyses.

Bishop Tuff, pyroxenes, magnetite, and biotite, all have rather similarly shaped light REE-enriched partition coefficient patterns with typical values of 5 to 20 for cerium and with Ce/Yb ratios commonly of 3 to 5. Bulk distribution coefficients for the high-temperature, allanite-free sample are about 0.9 for cerium and 0.1 for the heavy REE (6, 10). Michael (6) and Mittlefehldt and Miller (7) have pointed out that the addition of only trace quantities of allanite to the mineral assemblage will result in bulk distribution coefficients greater than 1 for cerium and neodymium and consequently depletion of the light REE with crystal fractionation.

If one determines bulk distribution coefficients of pumice samples by the "groundmass-mode" method (10), one avoids uncertainties encountered by Michael (6), arising from estimating the amounts of accessory minerals, estimating mineral/melt partition coefficients, using average compositions, and assuming that whole-rock (nonpumice) compositions represent the compositions of liquids. Using "groundmass-mode" bulk distribution coefficients and the Rayleigh equation, I find that the REE pattern of the medium-temperature pumice can be modeled by subtraction of 23 percent crystals (that is, 0.77 weight-fraction liquid remaining) from the parent high-temperature pumice. The low-temperature pumice can be modeled by subtraction of 42 percent crystals (that is, 0.58 weight-fraction liquid remaining) from the medium-temperature pumice. Thus the REE calculations suggest about 55 percent fractionation (that is, 0.45 weight-fraction liquid remaining) is required to derive the low-temperature pumice from a magma similar in composition to the high-temperature sample. The strontium isotopic diagram for the Bishop Tuff presented by Hildreth (3) requires some assimilation to accompany fractional crystallization. The REE were probably less sensitive to assimilation than strontium because there was less of a concentration difference between the magma and the wall rock for the REE than for strontium.

The major conclusion from these analyses is that the Bishop Tuff "early/late" REE trend reported by Hildreth mimics the groundmass/whole-rock relations of allanite-bearing pumice; that is, more differentiated rocks differ from less differentiated rocks as the groundmass differs from the whole rock in a single sample. Thus the trend reported by Hildreth is precisely that expected to result from crystal fractionation, and there is no need to invoke liquid-state differenti-

ation to explain the REE geochemistry of the Bishop Tuff.

Hildreth (1) emphasized that the chemical gradients in the Bishop Tuff magma chamber were established before crystallization of the phenocrysts found in the rocks. The results of this study indicate that the REE gradients in the magma chamber could be the result of fractionation of phases similar in mineralogy and in relative proportion to those found in the rocks. Hildreth has convincingly demonstrated that crystals neither settled nor floated in the magma chamber. The mechanism of crystal fractionation remains speculative; it may, however, involve precipitation or accretion, or both, of crystals onto the chamber walls.

KENNETH L. CAMERON

Board of Earth Sciences,
University of California,
Santa Cruz 95064

References and Notes

1. W. Hildreth, *Geol. Soc. Am. Spec. Pap.* 180 (1979), pp. 43-75.
2. ———, thesis, University of California, Berkeley (1977).
3. ———, *J. Geophys. Res.* 86, 10153 (1981).
4. G. Mahood and W. Hildreth, *Geochim. Cosmochim. Acta* 47, 11 (1983).
5. C. R. Bacon, R. A. Macdonald, R. L. Smith, P. A. Baedeker, *J. Geophys. Res.* 86, 10223 (1981); H. R. Crecraft, W. P. Nash, S. H. Evans, *ibid.*, p. 10303; A. Ludington, *ibid.*, p. 10423.
6. P. J. Michael, *Geology* 11, 31 (1983).
7. D. A. Mittlefehldt and C. F. Miller, *Geochim. Cosmochim. Acta* 47, 109 (1983).
8. C. E. Leshner, D. Walker, P. Candela, J. F. Hays, *Geol. Soc. Am. Abstr. Programs* 14, 545 (1982); C. E. Leshner and D. Walker, *Eos Trans. Am. Geophys. Union* 64, 883 (1983).
9. The high-temperature sample (HB77) was collected from Hildreth's (2) locality B77. Likewise, the low-temperature (HB52) and medium-temperature (HB133) samples are from Hildreth's localities B52 and B133, respectively. The pumice blocks came from nonwelded or

slightly welded deposits. Sample HB77 is from a single block 45 cm in diameter, but samples HB133 and HB52 are composites, each consisting of three to five identical appearing smaller pumice blocks collected from within a few meters of one another. Hematite-stained alteration rinds were cleaned from the specimens, and only the fresh white interiors were analyzed. After crushing, the samples were split. One aliquot was set aside for the whole-rock analysis, and the other was used for separation of groundmass glass. The glass was concentrated with the use of heavy liquids and a Franz isodynamic separator, and then it was hand-picked free of impurities under a microscope.

10. Bulk distribution coefficients can be calculated by two methods. In the "mineral-mode" method,

$$D_a = X_1 * K_1 + X_2 * K_2 + \dots$$

where D_a is the bulk distribution coefficient of element a , X_1 is the weight fraction of phase 1 in the mineral assemblage, and K_1 is the crystal/melt partition coefficient of element a for phase 1. Alternately, D_a can be calculated by the "groundmass-mode" method where

$$D_a = \frac{C_i}{C_i(1-F')} - \frac{F'}{(1-F')}$$

and F' is the weight fraction of liquid remaining (that is, weight-fraction groundmass in the mode), C_i is the concentration of element a in the original melt (in the whole rock), and C_i is the concentration of element a in the fractionated liquid (in the groundmass). Because there is considerable uncertainty in estimates of the modal amounts of accessory minerals, bulk distribution coefficients are calculated with the greatest confidence by the "groundmass-mode" method. The high- and low-temperature samples contain about 0.79 and 0.83 weight-fraction groundmass glass, respectively. These data, when combined with those from Table 1, yield $D_{Ce} = 0.88$, $D_{Nd} = 0.78$, $D_{Sm} = 0.52$, $D_{Eu} = 3.0$, $D_{Gd} = 0.31$, $D_{Dy} = 0.10$, $D_{Er} = 0.19$, and $D_{Yb} = 0.12$ for the high-temperature sample and $D_{Ce} = 1.86$, $D_{Nd} = 1.39$, $D_{Sm} = 0.71$, $D_{Eu} = 3.4$, $D_{Gd} = 0.31$, $D_{Dy} = 0.11$, $D_{Er} = 0.07$, and $D_{Yb} = 0.12$ for the low-temperature sample.

11. I thank G. Hanson for providing access to the isotope laboratory at the State University of New York, Stony Brook; J. Whitlock who prepared the glass separates; and J. B. Gill, M. G. Sawlan, and D. E. Sampson who made suggestions for manuscript improvement. A grant from the Faculty Committee on Research, University of California at Santa Cruz, supported the REE analyses. Field collecting expenses were defrayed by a grant from Institute of Geophysics and Planetary Physics, University of California, Los Angeles; Los Alamos National Laboratory; and the University of California.

24 February 1984; accepted 18 April 1984

The Association of Iron and Manganese with Bacteria on Marine Macroparticulate Material

Abstract. Evidence of *in situ* metal (iron and manganese) deposition onto bacteria associated with rapidly sinking particles in the open ocean is reported. Below 100 meters, bacteria are found with extracellular capsules containing metal precipitates; the frequency of these capsules increases with depth. The capsular metal deposits appear to contribute a major portion of the weakly bound fraction of the particulate iron flux.

Microbes have frequently been implicated in the phase changes (for example, from dissolved to solid) and redox transformations of metals such as iron and manganese in soils (1), springs, streams, and lakes (1-5). Although bacteria capable of oxidizing manganese in culture have been reported from seawater (2, 6), evidence of their *in situ* activity in marine environments has thus far been found only in sediments and certain

stratified areas such as Saanich Inlet (a British Columbian fjord with seasonally anaerobic conditions in its deep waters) (2, 7), in hydrothermal vent systems (8), and possibly in ferromanganese nodules (2, 9), but not in pelagic environments. We report here the discovery of iron and manganese deposits associated with bacteria commonly found with macroparticulate material in the oceanic water column. Our distributional data and a